Supplementary material (ESI) for Chemical Communications

Supporting Information

Stabilization of CeO_2 nanoparticles in a CO_2 rich solvent

Martin J. Hollamby[§], Kieran Trickett[§], Ana Vesperinas[§], Carl Rivett[‡], David C Steyler[‡], Zoe Schnepp[§],

Jon Jones[§], Richard K Heenan[†] Robert M Richardson[+], Otto Glatter[$] and Julian Eastoe*[§]

[§]*School of Chemistry and Department of Physics[+] University of Bristol, Cantock's Close, Bristol, BS8 1TS, UK*

[‡] *School of Chemical Sciences and Pharmacy, University of East Anglia, Norwich, NR4 7TJ, UK*

[†]*ISIS Pulsed Neutron & Muon Source, Rutherford Appleton Laboratories, Chilton, Didcot, OX11 0QX, UK*

[$]*Karl-Franzens Universität Graz, 8010 Graz, Austria*

**Corresponding author. E-mail: Julian.Eastoe@bristol.ac.uk*

Experimental

Chemicals and Materials. Cerium nitrate ($Ce(NO_3)_3.6H_2O$, 99%, Sigma-Aldrich) and ammonia solution (NH_3, 35%, Fisher Scientific) were used without further purification. Heptane was purchased from Fisher Scientific and purified by passing through chromatographic silica (Silica 60A, chromatography grade, Fisher Scientific). H_2O was of ultra-high purity (Elga Maxima or Millipore Milli-Q Plus system). Sodium dioctyl sulphosuccinate (AOT, 99%) was purchased from Aldrich and purified by Soxhlet extraction with ethyl acetate, followed by several centrifugation cycles in methanol to remove residual salt contaminants[1]. TC14 was synthesized and purified using methods detailed elsewhere.[2]

Preparation of CeO_2 Nanoparticles. Surfactant-stabilized nanoparticles (NPs) were synthesized by drop-wise mixing of two transparent microemulsions ([AOT] = 0.1 mol dm^{-3}, w = 7 where w = [water]/[surfactant]); one containing $[Ce(NO_3)_3]_{aq}$ = 1.8 mol dm^{-3}, the other containing $[NH_3]_{aq}$ = 5.5 mol dm^{-3}). Reactions were carried out at 323 K, with vigorous stirring.

NP Characterisation. UV-vis absorption spectra of NPs were obtained using a Thermo Evolution 300 spectrometer with Vision Pro software. Transmission electron microscopy (TEM) images were obtained using a JEOL JEM 1200 EX Mk. 2 microscope operating at 120kV with attached digital camera. High resolution (HR) TEM micrographs were obtained using a JEOL TEM 2010 operating at 200kV. Theoretical values for d-spacings (table S1) are sourced from the Crystallographic and Crystallochemical Database for Mineral and their Structural Analogues, available online at http://database.iem.ac.ru/mincryst/index.php (WWW-MINCRYST, CERIANITE-(Ce)-800). A number of SAED patterns were obtained and analyzed to obtain the experimental d-spacing values in table S1. Theoretical interatomic distances for CeO_2 are 2.3 Å for Ce – Ce and 2.7 Å for O – O; experimentally obtained values of 2.8 ± 0.4 Å (TC14-coated) from HRTEM fringes agree well with these.

Small-angle Scattering. Small-angle X-ray scattering profiles were initially obtained with a NanoSTAR (Bruker AXS), using Cu radiation produced in a sealed cathode tube (current = 35 mA, potential difference = 40 kV), focussed by cross-coupled Göbel mirrors arranged such

that radiation is monochromated to K_α = 1.54Å and collimated by a 300μm pinhole. The sample holder was a 1mm quartz capillary which was filled with the samples using a syringe. The sample chamber and beam path is evacuated to 10^{-2} bar during measurements. The detector is comprised of a concave Be entrance window, primary beam stop of white gold and a "proportional" chamber containing a high-pressure (4 bar) Xe gas mixture, converting captured photons to induced charges on a 2D multiwire grid detector. Scattering. SAXS experiments were also carried out on a purpose-built diffractometer at the University of Bristol, as decribed elsewhere.[3] Analysis was carried out using the FISH fitting program,[4] and a Schultz distribution of polydisperse spherical particles1 was found to provide an appropriate model. In all cases the polydispersity index was held at 0.3 (in line with findings by TEM; samples are polydisperse – see figure S1). Average radii from fits are given in table 1 of the main paper. Other more sophisticated methods (for example a core-shell or a bimodal type P(Q)) were also found to adequately model the data. However, given that SAXS is being used primarily to determine particle size it was decided to keep to the more parametrically simple model. Fitted SAXS profiles are shown in figure 2. Average particle diameters from fitting are summarised in table 1.

SANS experiments were carried out on the time-of-flight LOQ instrument at ISIS, UK where incident wavelengths are $2.2 \leq \lambda \leq 10$ Å, resulting in an effective Q range of 0.009–0.249 $Å^{-1}$. A D_2O droplet core was employed to provide contrast against the H-surfactant and H-solvent. Absolute intensities (±5%) for I(Q) (cm^{-1}) were determined by calibrating the received signal for a partially deuterated polymer standard. The samples were loaded on to an automatic sample changer and held a temperature of 25ºC. The measurements were corrected for empty cell (1 mm SANS cuvette), solvent background and transmission of each sample. Data analysis again employed the FISH fitting program[3] and a Schultz distribution of polydisperse spherical particles was found to provide the best fits, consistent with a large

body of published work on related systems.[1] In this case the polydispersity index was held at a value of 0.2. Fitted SANS profiles are shown in figure S3. Average radii from fits are given in table 1. The droplet diameter of $Ce(NO_3)_3$ -containing AOT-stabilised microemulsion is a little lower than that usually found for AOT-stabilised microemulsion droplets.[1] One possible explanation for this could be the ionic strength effect inside water pools, lowering the effective droplet size as previously observed for NaCl.[5]

Studies with CO_2. Phase behavior of NP samples in both pure CO_2 and 9:1 CO_2:heptane was carried out using a 10 ml custom-built high pressure cell (University of East Anglia, UK), equipped with two sapphire windows and a magnetic stirrer bar (a detailed description can be found elsewhere).[6] NP samples initially were placed directly into the cell and heptane, if required, was added by syringe. The quantity of added solid (NPs + surfactant) was kept constant at 0.061g (approximately equivalent to 0.0125 mol dm^{-3} surfactant, well below the solubility limit of TC14 alone).[2] The dry solid was calculated to contain 4% by weight NPs, so this value corresponds to 2.5 mg nanoparticles (or 0.25 g dm^{-3}). The cell was then sealed and cooled to 15 °C using a re-circulating water bath and placed on a high power magnetic stirrer plate. Liquid CO_2 was then distilled into the cell from a cylinder, via a valve near the bottom of the cell, and residual air bled out from an upper value to ensure complete filling with CO_2. The temperature was altered using the water bath; the cell pressure was controlled using a manual hydraulic pump, which regulated the height of a sealed piston (changing pressure through changes in cell volume), and measured using a pressure transducer. A rise for 60 bar to 350 bar at 288 K corresponds to an increase in density from 0.84 to 1.02 gcm^{-3}; therefore concentrations and mixed solvent compositions will increase by this factor of 20% over the pressure range between sample preparation (60 bar) and measurements (300 bar). Pressure-induced cloud points were determined by increasing pressure until the stirred

mixture was optically transparent, and then slowly lowering pressure until the rapid onset of a clear-to-opaque transition (cloud point, P_c). UV measurements were taken through the cell windows using a Hewlett Packard HP 8472 single-beam diode-array spectrometer. For these latter measurements, samples were delivered via a gauze cradle suspended from the cell piston (well above the windows), designed to only allow fully dispersed nanoparticles into the cell. This was to ensure no coating of cell windows by vigorously stirred, but non-dissolved, nanoparticles which could potentially give false UV readings. Insoluble nanoparticles, which were not incorporated into the solvents, remained in the upper gauze cradle.

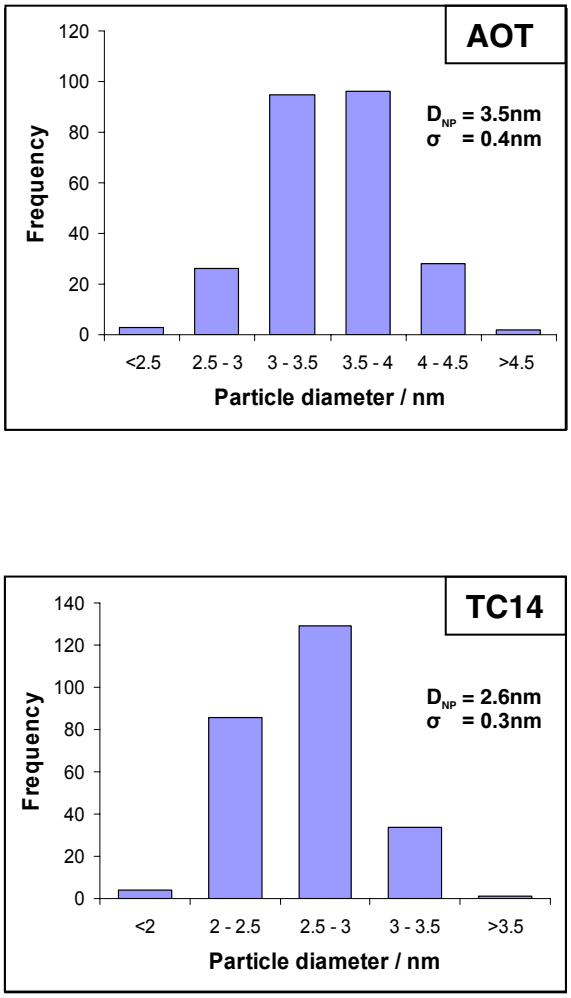

Figure S1. Bar charts showing particle diameter distributions for both AOT- and TC14-coated CeO_2 NP samples elucidated by size analysis of TEM images shown in figure 1 of the main paper. Numerical values for mean particle diameter (D_{NP}) and standard deviation (σ) are given in both cases.

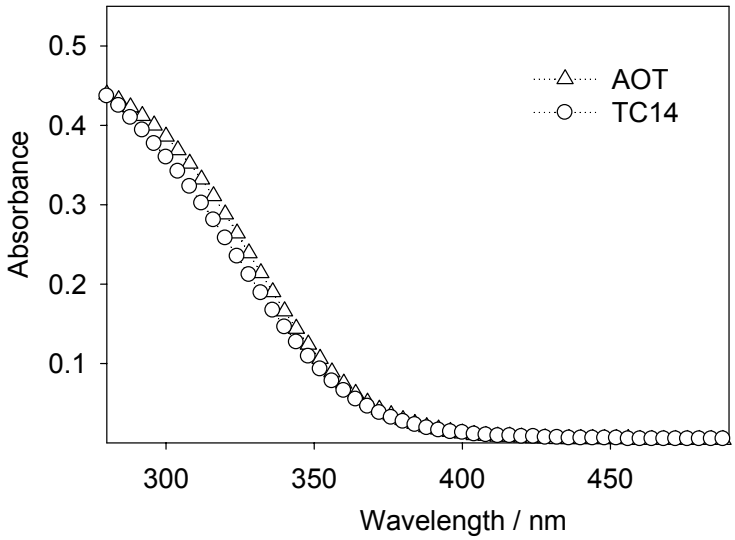

Figure S2. UV-vis absorption spectra of AOT- and TC14-coated CeO_2 NPs in heptane.

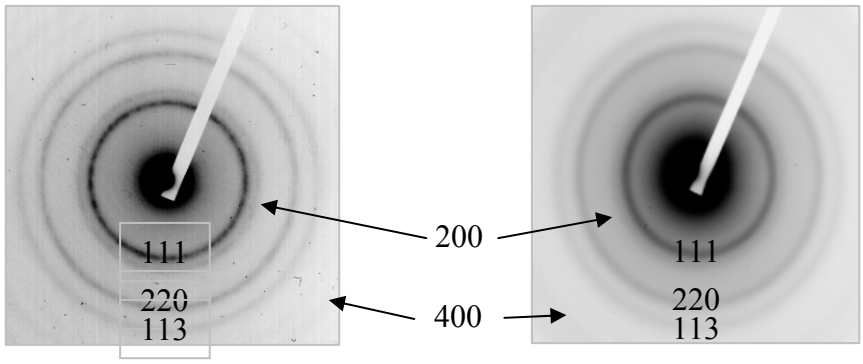

Figure S3. Example SAED patterns for AOT- (left) and TC14-coated (right) CeO_2 NPs, with visible rings marked with corresponding crystal lattice planes. Note both rings corresponding to (200) and (400) planes appear very faintly on these particular patterns.

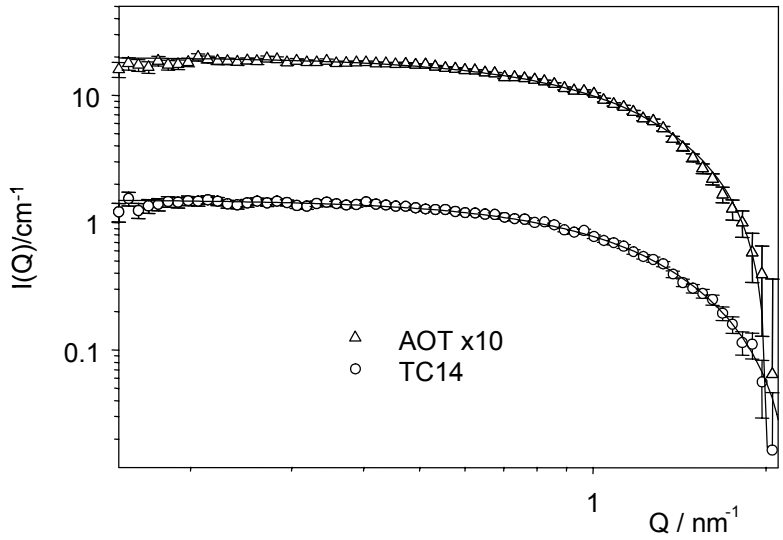

Figure S4. SANS profiles of the droplet core of AOT- and TC14-stabilised water-in-heptane microemulsions containing $Ce(NO_3)_3$ at [surfactant] = 0.1 mol dm^{-3}, w = 7 . Note I(Q) has been phase shifted by a factor of 10 for clarity. Lines show model fits.

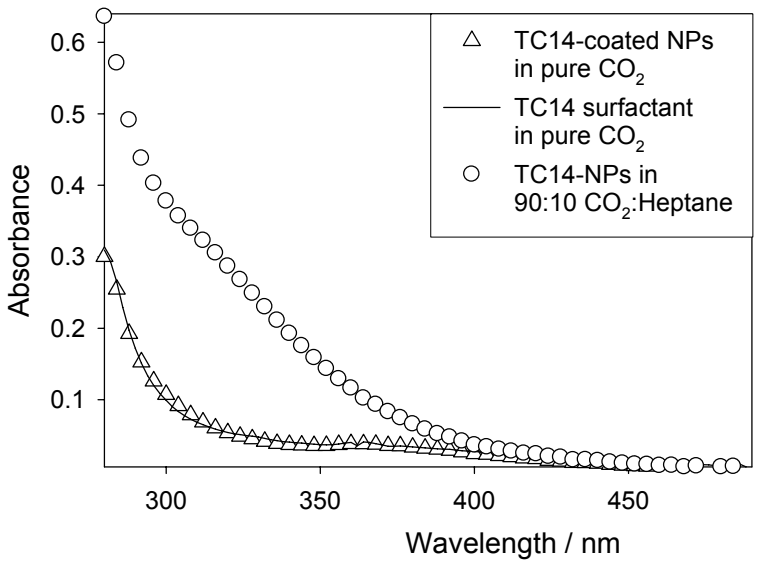

Figure S5. UV-vis absorption spectra of TC14-coated CeO_2 NPs in pure CO_2 and 9:1 CO_2:heptane.

The absorption spectrum of free TC14 surfactant in pure CO_2 is included for reference. Note the similarity between this UV-vis profile and that corresponding to TC14-coated CeO_2 NP's with the pure CO_2 solvent. The spectra are broadly identical, indicating that the UV absorption seen for the NP-containing sample corresponds to free TC14 surfactant (i.e. not including any of the CeO_2 NP's).

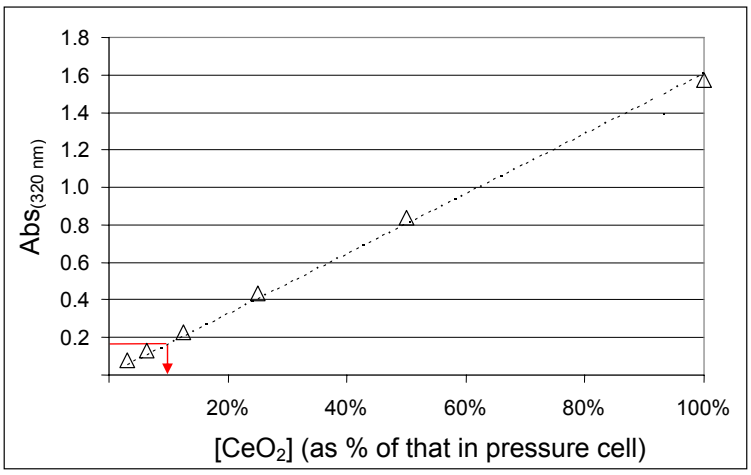

Figure S6. UV-vis absorbance at 320 nm ($Abs_{(320\ nm)}$) of CeO_2 NPs in heptane as a function of concentration. The pathlength-corrected absorbance at 320nm is equal to 0.17 for TC14-coated CeO_2 NPs in 9:1 CO_2:heptane, which as depicted corresponds to 10% of the CeO_2 initially entered into the gauze cradle.

H K L	d(theor) / Å	d(exp) / Å
1 1 1	3.12	3.03
2 0 0	2.70	2.67
2 2 0	1.91	1.82
1 1 3	1.63	1.57
4 0 0	1.35	1.24

Table S1. Comparison of d-spacing values obtained by SAED analysis and theoretical values for the fluorite structure of CeO_2.

References

1. S. Nave, J. Eastoe, R. K. Heenan, D. C. Steylter, I. Grillo, *Langmuir* 2000, **16**, 8741
2. S. Gold, J. Eastoe, R. Grilli, D. C. Steytler, *Colloid. Polym. Sci.* 2006, **284**, 1333
3. M. Summers, J. Eastoe, R. M. Richardson, *Langmuir* 2003, **19**, 6357-6362
4. R. K. Heenan, *FISH Data Analysis Program*; Rutherford Appleton Laboratory Report RAL-89-129, Didcot, U.K., 1989.
5. P. D. I. Fletcher, *J. Chem. Soc., Faraday Trans. 1* 1986, **82**, 2651
6. J. Eastoe, B. Robinson, D. C. Steytler, *J. Chem. Soc., Faraday Trans.* 1990, **86**, 511